Microstructures and high temperature mechanical properties of electron beam welded Inconel 718 superalloy thick plate

GAO Peng[1], ZHANG Kai-feng[1], ZHANG Bing-gang[2], JIANG Shao-song[1], ZHANG Bao-wei[1]

1. National Key Laboratory of Precision Hot Processing of Metals,
Harbin Institute of Technology, Harbin 150001, China;
2. State Key Laboratory of Advanced Welding and Joining,
Harbin Institute of Technology, Harbin 150001, China

Abstract: The microstructures and high temperature mechanical properties of whole and slices in Inconel 718 thick plate joint obtained by electron beam welding (EBW) were studied. The results show that, in the joint welded by full and cosmetic penetration, dendrites preserve in the top and bottom of welding center and columnar crystals emerge in the middle. The grain size in heat affected zone (HAZ) becomes smaller and smaller from top to bottom of welding line. The δ-phase precipitate in grain boundary and γ''-phase is obtained inside the grain of EBW joint, which was heat-treated with solution and double aging. The most of δ-phases appear in the weld center and the less turn up in HAZ and base material zone (BMZ). The tensile strength σ_b, yield strength σ_s and elongation δ of the whole joint at 650 °C are 1 100 MPa, 800 MPa and 18%, which reach 90%, 80% and 80% of base material's, respectively. The maximum σ_b, σ_s and δ lie in the bottom of joint and attain 1 170 MPa, 870 MPa and 18%, separately, while the minimum σ_b, σ_s and δ appear in the top of joint and reach 1 080 MPa, 780 MPa and 7%, respectively. The fracture of top weld is brittle; however, the ones of middle and bottom joint are flexible. The microhardness in HAZ and BMZ is higher than that in weld center. The value of microhardness tends to be lower as more δ-phase.
Key words: Inconel 718 superalloy; thick plate; electron beam weld; microstructure; high temperature mechanical property

1 Introduction

Inconel 718 is a nickel-based austenitic superalloy, which is strengthened primarily by γ''-Ni$_3$Nb and complementally by γ'-Ni$_3$(Al, Ti, Nb) [1]. Because of its superior properties, such as high temperature strength, high stability, antioxidation, irradiation, good hot-working character and weldability [2−3], Inconel 718 has become the key material in aviation, aerospace and nuclear energy fields [4−5]. In particular, the thick plate components of Inconel 718 have a good application prospect in industrial field. Besides the advantages of Inconel 718, it still has good properties for high rigidity, wear resistance and long life. For the thick plate, the influences of welding joint are very important to the components quality. Due to a great deal of elements and precipitated phases under heating conditions, Inconel 718 is sensitive to heat input. Meanwhile, connecting the thick plate, the large ratio between width and depth is required. EBW has a lot of advantages including large density of heat input, focused power, narrow heat affected zone, little weld thermal deformation, small ratio between width and depth, and excellent joint [6−7]. Therefore, it can satisfy the need of thick plate welding.

In recent years, scholars have conducted some research on organization performance of EBW and thick plate welding. HUANG et al [8−9] focused on the research of microstructure and galvanic corrosion behavior of heat affected zone of Inconel 718 thick plate after EBW. FERRO et al [10] studied EBW process for 10 mm-thick plate of Inconel 706 and analyzed the influence of weld heat input on the joint's microstructure. VISHWAKARMA et al [11] observed and studied the microstructure of weld fusion and heat affected zone in 15.9 mm-thick plate joint of an improved Inconel 718 (718 Plus) using transmission electron microscopy techniques. SARESH et al [12] carried out the systematic experiments, explored and summarized the EBW process of 21 mm-thick Ti-6Al-4V. XU et al [13−14] studied the microstructures of welded nugget zone (WNZ) and mechanical properties of whole specimen and slice in the

Corresponding author: ZHANG Kai-feng; Tel: +86-451-86418763; E-mail: kfzhang@hit.edu.cn

14 mm-thick aluminum plate obtained by friction stir welding.

It is noted that, during connecting the thick plate by EBW, obvious temperature gradient along the direction electron beam and differences in the heat inputs of weld depth direction generates, which results in the uneven microstructure and mechanical properties of joint. By now, there is less research about microstructure and high temperature mechanical properties of whole specimen and slice in Inconel 718 thick plate.

2 Experimental

The as-received Inconel 718 was in the form of 12 mm×200 mm×100 mm hot rolled plates with a chemical composition shown in Table 1. The original microstructure of the plates with grain size of 20−30 μm is shown in Fig. 1. Electron beam welding in vacuum was carried out on equipment of KL110 produced in Ukraine. Welding direction was along the length of joint and butt welding was accomplished. Welding sample was fixed by special fixture. In order to obtain a joint with good surface quality, the gap between connecting boundaries of specimens must be less than 0.1 mm. Therefore, the joint face and top surface close to welding line were machined by CNC machining centre. Then, the welding samples were cleaned by acetone. In order to prevent the top surface of welding line from sinking, EBW process used in this study included two steps: full penetration and cosmetic penetration. The welding parameters are shown in Table 2.

Table 1 Chemical composition of Inconel 718 thick plate used in this study

Element	Mass fraction/%
C	0.027
Mn	0.02
Si	0.08
S	0.001
P	0.004 5
Ni	52.32
Cr	18.53
Mo	3.03
Cu	<0.07
Ti	1.06
Al	0.50
B	0.001 6
Co	0.035
Nb+Ta	5.19
Fe	Bal.

After EBW operation, the Inconel 718 un-welded thick plates and welded plates were heat treated by solution and double aging. The solution-treatment was carried out at 980 °C for 1 h with air cooling. In addition, the first aging was put into effect at 720 °C for 8 h and the specimens were cooled in furnace at 50 °C/h. The second aging was executed at 620 °C for 8 h and then specimens were cooled in air.

Fig. 1 Original microstructure of Inconel 718 hot rolling thick plate

Table 2 Welding parameters of EBW used in this study

Welding pass	Voltage/ kV	Focus current/mA	Current/ mA	Feed/ (mm·s⁻¹)
First pass (full penetration)	60	700	120	11
Second pass (cosmetic penetration)	60	700	30	11

The joints were cut into slices along the section which was perpendicular to the welding direction. After being mechanically grinded and polished, metallographic specimen was corroded by mixed acid solution (2 mL HF+20 mL HNO_3+100 mL HCl+76 mL H_2O). Then, it was observed on a microscope of LEXT-OLS3000 to analyze its microstructure. The heat treated whole specimen and slices (three specimens either) of Inconel 718 un-welded plates and EBW joints were drawn at 650 °C (usage temperature of Inconel 718) by Instron5500R electronic material testing machine. The size of drawn samples is shown in Fig. 2. The unsmooth surfaces of EBW joints were wiped off. Analysis for fracture surface of drawn specimens and precipitated
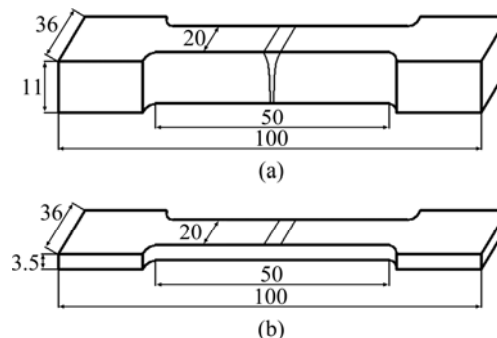

Fig. 2 Dimensions of whole (a) and slice (b) of tensile sample (mm)

phase in the microstructure of joints was achieved by FEI Quanta 200F scanning electron microscope (SEM). After being observed by FEI TECNHI G2 F30 transmission electron microscope (TEM), the crystal structure of precipitated phase was calibrated by its electronic diffraction pattern. After that, the microhardness of welded section on the top, middle and bottom joint was measured by HVS−1000Z. The gap between two test points was 0.5 mm, testing load was 9.8 N and loading time was 15 s.

3 Results and discussion

3.1 Microstructure

Figure 3(a) shows the EBW joint section of Inconel 718 superalloy after heat treatment. This shows the keyhole-shape and the microstructure are as cast organization. The welded section is divided into three parts to observe: the top, middle and bottom level. Figs. 3(b)−(g) show the microstructures corresponding to the position of the black box in Fig. 3(a).

Figure 3(b) shows the microstructure at the top of weld center, in which EBW process was carried out by full and cosmetic penetration. Because the position of cosmetic penetration is close to the surface of plate, the cooling speed is fast after joint welded. This result in the recrystallization dentrites crystal formed at this position is preserved. The welding beam of cosmetic penetration is only 25% of joint welded. Kinetic energy of electron beam is small and heat input concentrates in the top weld. Consequently, in Fig. 3(e), compared with primitive grain, the grain size of heat affected zone near fusion line grows up obviously. And the gradient of top weld fusion line is larger, cross-section of metal melting zone is approximate fan-shape. Compared with top weld, the number of dentrites in middle weld center (Fig. 3(c)) is small, and that of columnar grain is large. This middle center lies in the middle of the plate thickness direction, so, after joint is welded, compared with plate surface, the cooling speed is slow. This provides conditions for the formation of columnar crystal inside fusion line, which leads to the number of dentrites in center place decreasing. The grains in the middle of weld heat affected zone (Fig. 3(f)) also have grown up, but are also smaller than the corresponding ones at the top. The reason is although the cooling speed in middle joint is
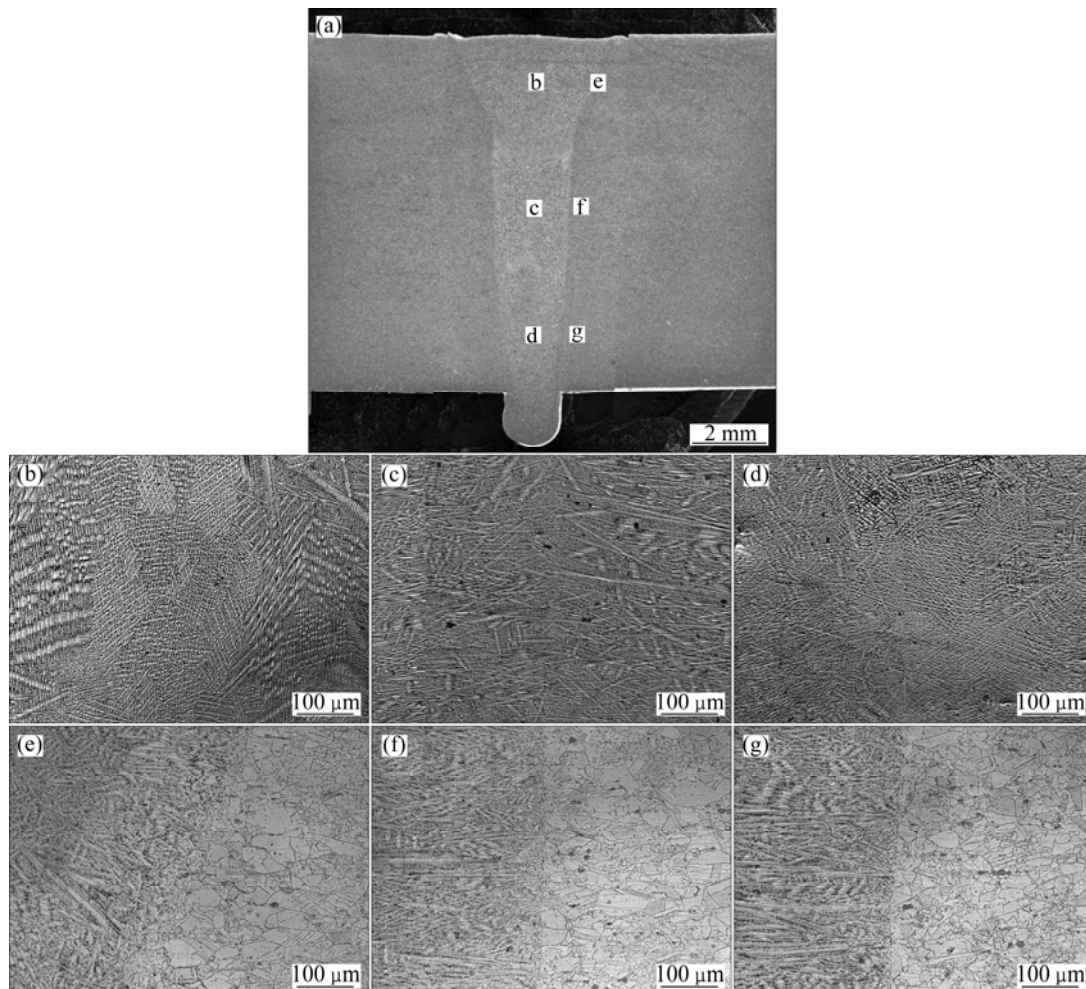

Fig. 3 Microstructures of EBW joint (a) and top (b), middle (c) and bottom (d) of weld center and top (e), middle (f) and bottom (g) of heat affected zone

less than plate surface, cosmetic penetration does not perform in this area, so that the total heat input of EBW is still less than that on surface. Similar with the top, a certain amount of dentrites crystal is preserved at the bottom of weld center (Fig. 3(d)). Compared with original plate, grains in the bottom heat affected zone (Fig. 3(g)) do not grow up obviously. After welding penetration, cooling speed of the area near the lower plate surface is fast, resulting in that tiny grain retains at weld center, and the growth of grain in heat affected zone is inhibited.

3.2 Precipitated phase

Morphologies of precipitated phase in Inconel 718 EBW welded joint after heat treatment are shown in Fig. 4. Figure 4(a) shows that the number of precipitated phase increases in the welded center of grain boundary, most of which appear in the form of rod, meanwhile, a small amount of precipitation gather up and grow up. As shown in Fig. 4(b), the precipitated phase in heat affected zone is less than that at weld center. However, amount of boundary phases in the adjacent zone of the fusion line are obviously precipitated with the density close to that in weld center. Figure 4(c) shows that the minimum precipitated phase exists in the base materials zone, most of which arrange along the grain boundary in the form of rod and a few appears in the form of fine granule. A large number of disperse granular phase with size of 20−30 nm is precipitated inside the grain of total joint. For example, Fig. 4(d) shows the intragranular precipitated phase in the weld center.

As shown in Fig. 5(a), the EBW joint is observed using transmission electron microscope and crystal structure of intergranular precipitated phase is calibrated by electron diffraction pattern (Fig. 5(b)). It shows that the precipitation is Ni_3Nb phase whose structure is HCP, which is named as δ-phase in Inconel 718 superalloy. This phase precipitates in grain boundary and plays a role in fixing grain boundary. It can effectively restrain the growth of grains in Inconel 718, leading to that the superalloy owns comprehensive mechanical properties [15]. Figure 5(c) shows the morphology of intragranular precipitated phase in EBW joint, which is calibrated as Ni_3Nb with the structure of BCT by electron diffraction pattern (Fig. 5(d)). This precipitation is the primary strengthening phase (γ''-phase) of Inconel 718, and precipitates inside the grains and makes the material own superior high temperature strength.

3.3 High temperature mechanical properties

Figure 6 shows the high temperature mechanical properties of tensile specimen of whole and slice in Inconel 718 thick plate EBW joints at its usage temperature of 650 °C. As shown in Fig. 6(a), the value of tensile strength σ_b of slicing joint gradually increases from top to bottom, the minimum value (top) is about 1 100 MPa and the maximum value (bottom) is close to 1 200 MPa. The tensile strength of the whole joint is
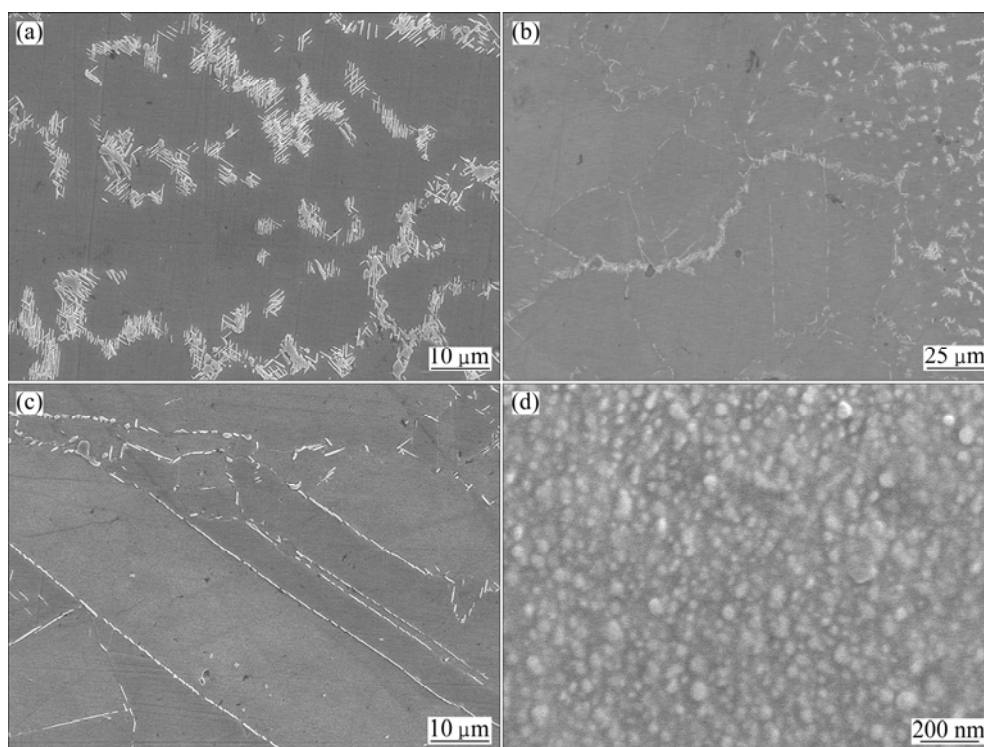

Fig. 4 Intercrystalline precipitated phases in weld center (a), heat affected zone (b), base metal zone (c) and intragranular precipitated phases in weld center (d)
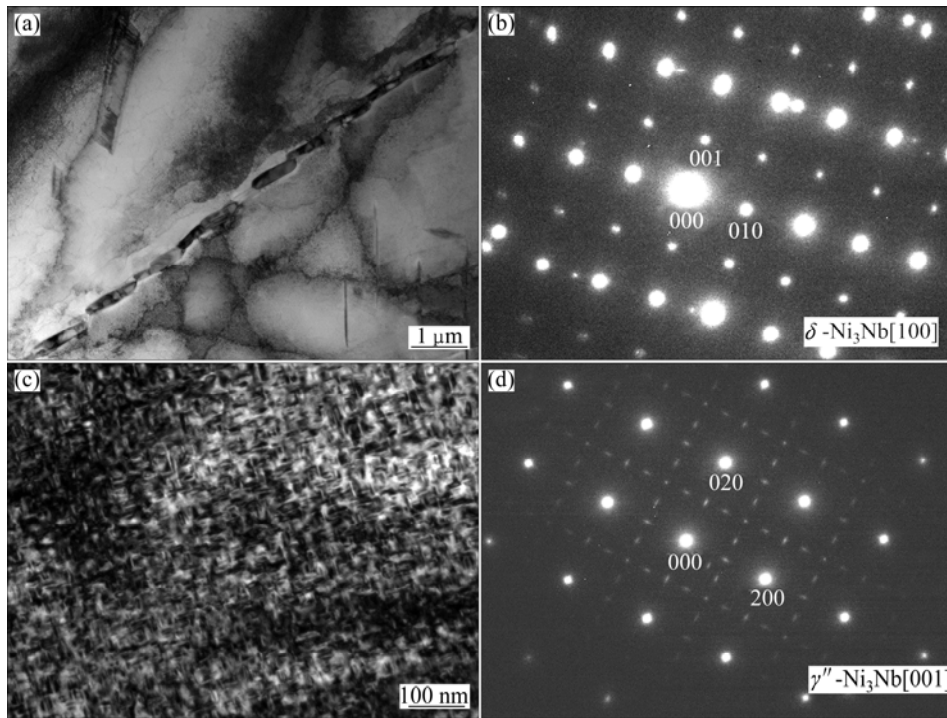
Fig. 5 TEM images of intercrystalline precipitated (a) and intragranular precipitated (c) phases and their electronic diffraction patterns (b, d)
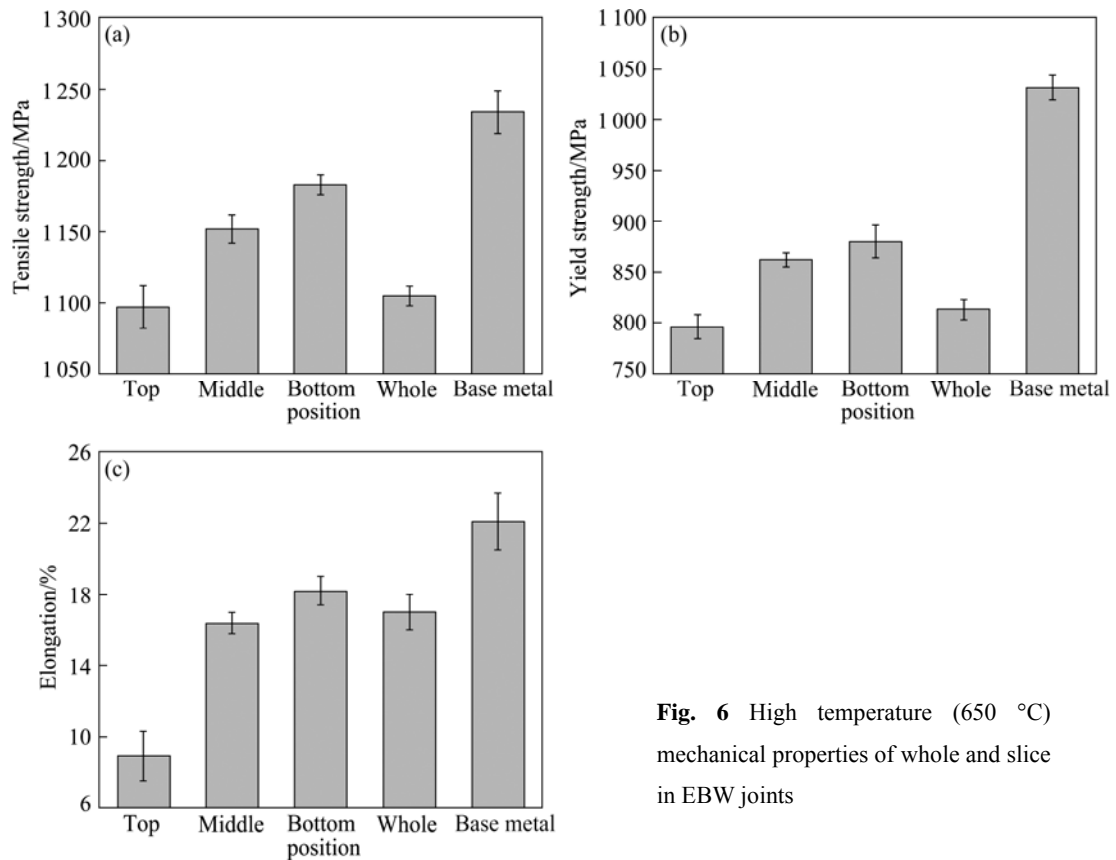

Fig. 6 High temperature (650 °C) mechanical properties of whole and slice in EBW joints

around 1 100 MPa, reaching 90% of base material's, approaching to the strength of the top section. Therefore, the tensile strength of the overall joints is the minimum

value of slices. Figure 6(b) shows that the trend of variation in yield strength σ_s is consistent with that of tensile strength. But the proportion between the yield

strength of whole joint and the base material decreases to 80%. The case of elongation δ is different from the ones of σ_s and σ_b, as shown in Fig. 6(c). Although the trend of δ of slices is the same as that of strength, the elongation of the top section is much lower than other layers, reaching only 40% of base material. The elongation of the whole joint is much higher than that value of top section, closing to the ones of the middle and bottom (about 80% of the base material). It can be concluded that, as the weak part of the EBW weld, the strength of the top slice determines the value of whole joint. Although the elongation of the top section is the lowest, when the top begins to crack, the EBW joint still does not break immediately because of the support of middle and bottom.

3.4 Fracture analysis

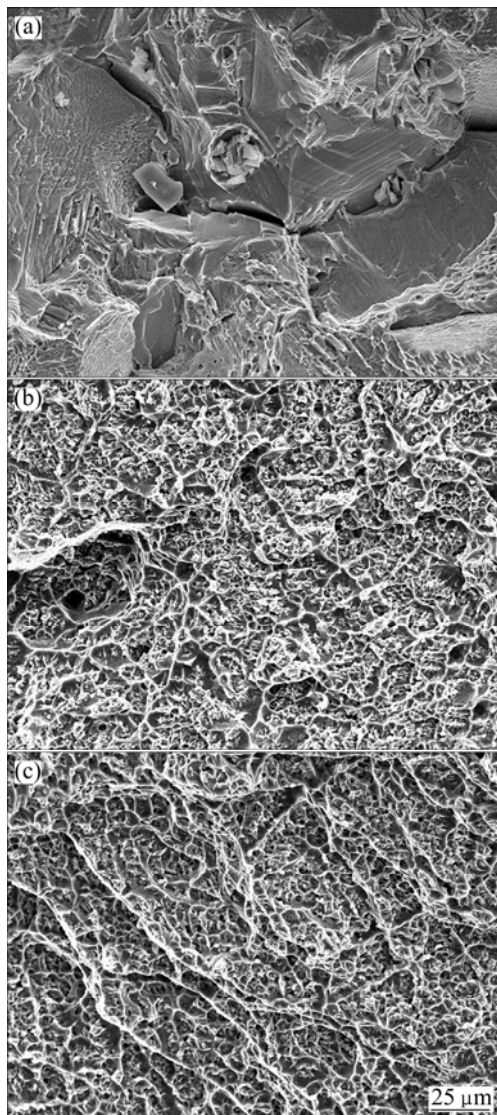Figure 7 shows the morphologies of tensile fracture of Inconel 718 EBW joint slices. Fracture position of the top sample locates in heat affected zone. However, the middle and bottom samples are broken in the center of the weld. As shown in Fig. 7(a), grain size of the fracture of top sample is the largest and most of fractures shows obvious features of cleavage fracture. It also can be seen that a few of broken second-phases emerge in the crack. Few small and shallow dimples appear in this region, which results in the lower extension of the top section. Figures 7(b) and (c) show that the dimples are dispersed throughout the fracture surface of middle and bottom joints, whose size is about 10 μm. And also the broken second-phase particles are visible inside dimples. This indicates that, in this region, the material mainly broke in the way of ductile rupture. As a result, their mechanical properties are better than top.

3.5 Microhardness

Figure 8 shows the distributions of test points and microhardness along the transverse section of slice in EBW joint. As shown in Fig. 8(b), the hardness in the welded center is the lowest, while that in the heat affected zone and base material is higher. To the slices, in the region of welded center, the microhardness of the middle section is higher than that of the other levels. However, the microhardness distribution of slices is not regular in heat affected zone and base material.
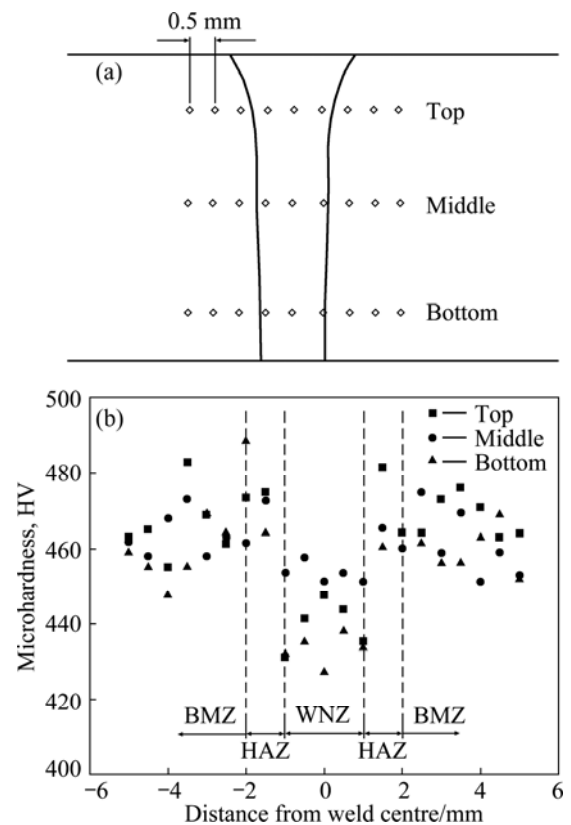

Fig. 7 Fractographs of top (a), middle (b) and bottom (c) in EBW joint

Fig. 8 Distributions of test points (a) and microhardness (b) along transverse section of slice in EBW joint

From the analysis of microstructure mentioned above, the smallest grains form in the center of weld because of recrystallization. And the biggest grains emerge in the heat affected zone caused by heat input of welding.

In general, the relationship between the hardness and grain size can be given mathematically by SATO et al [16]

$$H_V = H_0 + k_H d^{-1/2} \tag{1}$$

where H_V is hardness; d is grain diameter; H_0 and k_H are constants.

According to Eq. (1), the hardness increases with the grain size decreasing. It can be conducted that the hardness of weld should be the largest in the central area and the lowest in heat affected zone. However, the test result is opposite to the theoretical derivation. So, the further analysis is carried out. It is worth noting that the chemical composition of intercrystalline precipitation (δ-phase) is Ni_3Nb, which is consistent with that of intragranular precipitated phase (γ''-phase). Meanwhile, Nb is shared by δ-phase (Ni_3Nb), γ''-phase(Ni_3Nb) and γ'-phase (Ni_3(Al, Ti , Nb)). This means that once any of them increases, the other will decrease. As shown in Figs.4(a)−(c), the intercrystalline precipitation (δ-phase) in welded center is more than that in heat affected zone and base material, which indicates that intragranular precipitated phases (γ''-phase and γ'-phase) in weld center are less than these in heat affected zone and base material. This results in that the effect of precipitated strength in heat affected zone and base material is much better than that in weld center, making the higher microhardness in the former regions.

4 Conclusions

1) At the top and bottom of 12 mm-thick Inconel 718 plate EBW joints, dendrites preserve and the columnar grains emerge at the middle. In heat affected zone, the grain size decreases gradually from the top to the bottom.

2) At 650 °C, the maximum σ_b, σ_s and δ lie in the bottom of joint and attain 1 170 MPa, 870 MPa and 18%, separately, while the minimum σ_b, σ_s and δ appear in the top of joint and reach 1 080 MPa, 780 MPa and 7%, respectively. In middle and bottom slices, the material mainly breaks in the way of ductile rupture, while the fracture in the top shows obvious features of brittleness.

3) After solution and two-aging treatment, the δ-phase (Ni_3Nb) precipitates in the grain boundary. The quantity of them in weld center is much more than that in other regions, leading to that microhardness in this zone is the lowest. The reason is that once the precipitation of δ-phase increases, γ'' and γ' (strengthening phases of Inconel 718) will decrease because Nb is shared by all of them.

References

[1]   XIE Xi-shan, DONG Jian-xin, FU Shu-hong, ZHANG Mai-cang. Research and development of γ'' and γ' strengthened Ni-Fe base superalloy GH4169 [J]. Acta Metallurgica Sinica, 2010, 46(11): 1289−1305. (in Chinese)

[2]   THOMAS A, EL-WAHABI M, CABRERA J M, PRADO J M. High temperature deformation of Inconel 718 [J]. Journal of Materials Processing Technology, 2006, 177: 469−472.

[3]   YUAN H, LIU W C. Effect of the δ phase on the hot deformation behavior of Inconel 718 [J]. Materials Science and Engineering A, 2005, 408: 281−289.

[4]   HAN W B, ZHANG K F, WANG B, WU D Z. Superplasticity and diffusion bonding of IN718 superalloy [J]. Acta Metallurgica Sinica: English Letters, 2007, 20: 307−312.

[5]   WANHILL R J H. Significance of dwell cracking for IN718 turbine discs [J]. International Journal of Fatigue, 2002, 24: 545−555.

[6]   MAGNABOSCO I, FERRO P, BONOLLO F, ARNBERG L. An investigation of fusion zone microstructures in electron beam welding of copper-stainless steel [J]. Materials Science and Engineering A, 2006, 424: 163−173.

[7]   HO C Y. Fusion zone during focused electron-beam welding [J]. Journal of Materials Processing Technology, 2005, 167: 265−272.

[8]   HUANG C A, WANG T H, LEE C H, HAN W C. A study of the heat-affected zone (HAZ) of an Inconel 718 sheet welded with electron-beam welding (EBW) [J]. Materials Science and Engineering A, 2005, 398: 275−281.

[9]   HUANG C A, WANG T H, HAN W C, LEE C H. A study of the galvanic corrosion behavior of Inconel 718 after electron beam welding [J]. Materials Chemistry and Physics, 2007, 104: 293−300.

[10]   FERRO P, ZAMBON A, BONOLLO F. Investigation of electron-beam welding in wrought Inconel706 experimental and numerical analysis [J]. Materials Science and Engineering A, 2005, 392: 94−105.

[11]   VISHWAKARMA K R, RICHARDS N L, CHATURVEDI M C. Microstructural analysis of fusion and heat affected zones in electron beam welded ALLVAC® 718PLUS™ superalloy [J]. Materials Science and Engineering A, 2008, 480: 517−528.

[12]   SARESH N, PILLAI M G, MATHEW J. Investigations into the effects of electron beam welding on thick Ti-6Al-4V titanium alloy [J]. Journal of Materials Processing Technology, 2007, 192−193: 83−88.

[13]   XU Wei-feng, LIU Jin-he, LUAN Guo-hong, DONG Chun-lin. Microstructures and mechanical properties of friction stir welded aluminium alloy thick plate [J]. Acta Metallurgica Sinica, 2008, 44(11): 1404−1408. (in Chinese)

[14]   XU Wei-feng, LIU Jin-he, LUAN Guo-hong, DONG Chun-lin. Microstructures and mechanical properties of friction stir welded joints of aluminium alloy thick plate with different welding states [J]. Acta Metallurgica Sinica, 2009, 45(4): 490−496. (in Chinese)

[15]   SUNDARAMAN M, MUKHOPADHYAY P, BANERJEE S. Loria superalloys 718, 625, 706 and various derivatives [C]//Warrendale, PA: TMS, 1994: 419.

[16]   SATO Y S, URATA M, KOKAWA H, IKEDA K. Hall-Petch relationship in friction stir welds of equal channel angular-pressed aluminium alloys [J]. Materials Science and Engineering A, 2003, 354: 298−305.

Inconel 718 合金厚板真空电子束焊
接头的显微组织与高温力学性能

高 鹏[1]，张凯锋[1]，张秉刚[2]，蒋少松[1]，张宝为[1]

1. 哈尔滨工业大学 金属精密热加工国家重点实验室，哈尔滨 150001；
2. 哈尔滨工业大学 先进焊接与连接国家重点实验室，哈尔滨 150001

摘 要： 对 Inconel 718 高温合金 12 mm 厚板的真空电子束焊(EBW)接头整体及分层的显微组织和高温力学性能进行了研究。结果表明：经熔透焊+修饰焊的接头，焊缝中心的上、下层为树枝晶，中层为柱状晶；热影响区由上层至下层晶粒长大程度逐渐减小。经固溶+双时效热处理后，EBW 接头各区域晶界处均有 δ 相析出，在焊缝中心最多，在热影响区及母材较少，晶粒内部均析出了 γ'' 相。在 650 °C 时，接头整体的抗拉强度 σ_b、屈服强度 σ_s 和伸长率 δ 分别为 1 100 MPa、800 MPa 和 18%，达到了母材的 90%、80%和 80%。分层切片的力学性能下层最高，σ_b、σ_s 和 δ 分别达到了 1 170 MPa、870 MPa 和 18%；上层最低，分别为 10 80 MPa、780 MPa 和 7%。上层断口以脆性断裂为主，中、下层断口以韧性断裂为主。显微硬度分布为焊接中心最低，热影响区与母材较高。晶界 δ 相的析出数量越多，显微硬度值越低。

关键词： Inconel 718 高温合金；厚板；电子束焊接；显微组织；高温力学性能

(Edited by LI Yan-hong)